Adapting-Bump Model for Eccentric Cells of *Limulus*

FULTON WONG and BRUCE W. KNIGHT

From The Rockefeller University, New York, New York 10021. F. Wong's present address is the Marine Biomedical Institute, The University of Texas Medical Branch, Galveston, Texas 77550.

ABSTRACT Light-evoked intracellular voltage noise records have been obtained from *Limulus* eccentric cells, from threshold light intensity to an intensity $\cdot 10^5$ times threshold. These data are analyzed in terms of a simple "adapting-bump" noise model. It is shown how the model yields a data reduction procedure that slightly generalizes the familiar use of Campbell's theorem for Poisson shot noise: the correlative effect of adaptation amends Campbell's theorem by a single multiplicative factor, which may be estimated directly from the power spectrum of the noise data. The model also permits direct estimation of the bump shape from the power spectrum. The bump shape estimated from noise at dim light is in excellent agreement with the average shape of bumps observed directly in the dark. The data yield a bump rate that is linear with light up through about 50 times threshold intensity but that falls short of linearity by a factor of 35 at the brightest light. The bump height decreases as the -0.4 power of light intensity across the entire range. Bump duration decreases by a factor of 2 across the entire range, and the adaptation correlation factor descends from unity to about one-third. The modest change of the adaptation correlation shows that naive application of Campbell's theorem to such data is adequate for rough estimation of the model's physiological parameters. This simple accounting for all the data gives support to the adapting-bump model.

INTRODUCTION

The primary event in the phototransduction process is a light-induced isomerization of the photopigment. The mechanisms that link this event to the electrical response within the photoreceptor cell remain unknown. However, recordings of the slow receptor potential (generator potential) from *Limulus* photoreceptors have shown that the response to light is related to the occurrence of discrete events known as "quantum bumps" (Yeandle, 1957). These bumps are transitory increases in membrane conductance that lead to "waves" of depolarization (Adolph, 1964). Bumps have been observed in photoreceptors of several arthropods: *Locusta* (Scholes, 1965); *Musca* (Kirschfeld, 1966); ventral photoreceptors of *Limulus* (Millecchia and Mauro, 1969); *Drosophila* (Wu and Pak, 1975). The work of Fuortes and Yeandle (1964) and of Adolph (1964) shows that at very low light intensities the rate of appearance of the

J. GEN. PHYSIOL. © The Rockefeller University Press · 0022-1295/80/11/0539/19 $1.00 539
Volume 76 November 1980 539–557

bumps increases proportionally to light intensity. The times of occurrence of bumps, however, appear to be random and independent. Fuortes and Yeandle (1964) also suggested that each bump follows the absorption of a single photon. (See also Borsellino and Fuortes [1968].) The generator potential appears to be a summation of these quantum bumps (Rushton, 1961).

Fig. 1 shows further features of the intracellular voltage response to light. In steady state the generator potential does not increase proportionally to light

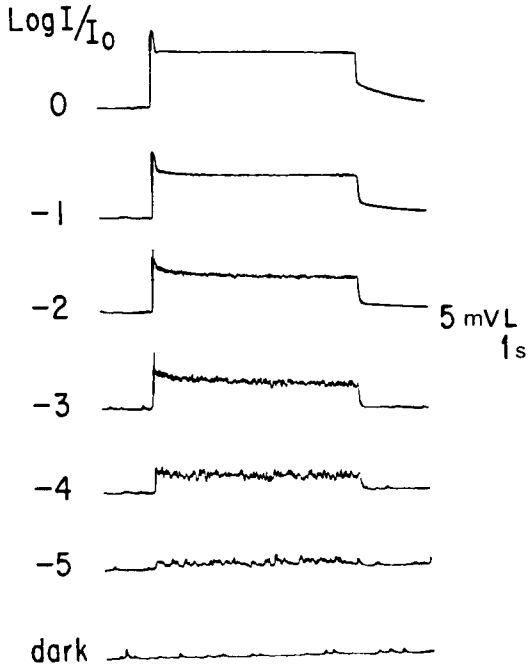

FIGURE 1. Records obtained from an eccentric cell showing the responses of a photoreceptor to light of various intensities. The lowest trace shows that, for a very dark-adapted cell, bumps could occur spontaneously in the dark. (The spontaneous bumps only occur when the cell is very dark adapted.) Under very dim, steady illumination (−5 log), it appears that the response is the sum of more frequent bumps. At higher light intensities, it is not possible to observe the bumps individually. There are three major features: first, in response to step changes of light intensity, the response goes through a transient phase and a smaller plateau, and the mean amplitude of the response in the steady state does not increase proportionally with light intensity but more as its logarithm. Second, the amplitude of the noise of the response decreases markedly with increasing light intensity. (If these responses were the summation of bumps such as those seen in dim light, and if the number of bumps per second increased proportionally with light intensity, one would expect to see the mean amplitude increase proportionally with light intensity; and the mean amplitude of the noise should also increase.) Third, there are no big bumps seen immediately after the cessation of a bright light. These observations suggest that the response to bright light is the sum of bumps the average size of which is smaller than the average size of the bumps seen in dim light.

intensity but more nearly as its logarithm. Moreover, the amplitude of the noise about the mean decreases with increasing light intensity (Dodge et al., 1968). After the onset of steady light, an early voltage transient settles back to a steady state, and, after bright light, a dim light evokes bumps of reduced size (Dodge et al., 1968). It is as though brighter light causes a superposition of smaller bumps. These observations may be summarized by two model postulates (advanced by Rushton [1961], Adolph [1964], and Dodge et al. [1968]): (*a*) the generator potential is a summation of bumps; and (*b*) the average size of bump decreases with light intensity, and this is the major mechanism of light adaptation. We shall call these postulates the "adapting-bump model."

If the voltage response in steady light results from the superposition of numerous bumps, its average value (in millivolts) should be the product of two more fundamental factors, the rate λ (in inverse seconds) at which new bumps appear and the "average bump size" s (in millivolts times seconds), which is the area under a typical bump if we plot its time-course as millivolts vs. time. There is a natural way (discussed below; Eqs. 3 and 4) to further resolve the bump size into two factors, its "height" (h, in millivolts) and its "duration" (T, in seconds, so that $s = h\mathrm{T}$).

(We note here that when we come to the analysis of actual data, we shall deal not with the observed variable, voltage, but with the more fundamental, derived biophysical variable, membrane shunt conductance, which differs from voltage by a simple transformation. We find that the material of the next paragraphs is most easily communicated in terms of the voltage variable, which is actually seen in the laboratory.)

Once a model of the photoresponse has been defined in sufficient detail, we may analyze experimental voltage noise records to extract the three underlying parameters of λ, h, and T. A rough analysis of this sort was reported without procedural details for voltage noise in *Limulus* visual cells by Dodge et al. (1968), who estimated the T from the voltage-frequency response to sinusoidally flickered light and then estimated λ and h by a direct application of Campbell's theorem. The use of Campbell's theorem (Rice, [1944]; see also Hagins [1965]) is a classic technique for extracting rate and height information from a "Poisson shot noise," which is a superposition of independent bumps.

The procedure of Dodge et al. (1968) is open to logical challenge in two respects. Firstly, it is now known (Wong et al., 1980) that the frequency response to flicker is not uniquely related to the bump shape but depends also on the "dispersion of latencies" between photon capture and bump release. (Dodge et al. [1968] mention that their analysis is limited to data for which such dispersion could be ruled out as a significant effect.) Secondly, the adapting feature of the adapting-bump model implies that the sizes of later bumps are reduced by (and hence correlated with) the capture of photons that have given rise to earlier bumps. The assumption of adaptation is not strictly consistent with the use of Campbell's theorem, which holds for a Poisson shot noise of uncorrelated bumps. (Dodge et al. mention that the effect of correlation shortens their calculated duration by a spurious factor of

up to 2. They give no guiding details but refer to work "in preparation," which now appears in Knight [1973]).

Our purpose here is to present and apply a method whereby the three parameters duration T, height h, and rate λ can all be estimated from steady voltage noise alone in a manner consistent with and correct for the adapting-bump model.

Theory

In this section we present Campbell's theorem, which leads us by a simple dimensional argument to natural expressions for the height and duration of a bump whose shape is arbitrary. Campbell's theorem takes a particularly simple form in terms of these parameters. Another simple dimensional argument shows how the correlation among bumps may modify Campbell's theorem only by the introduction of a single, dimensionless multiplicative factor. We then observe how the power spectrum of a noise composed of uncorrelated bumps is related to T; two procedures for estimating T are presented, one simple and the other more general. At this point, the data indicate that in bright light there is correlation among the underlying bumps in the voltage noise; the data also indicate where this correlation will modify the power spectrum. A quantitative estimate of this modification is made and is applied directly to evaluation of the correlation correction to Campbell's theorem, whereupon rate, height, and duration can be estimated for the correlated voltage noise.

If a random variable is the sum of underlying random variables, then, quite generally, its mean value is the corresponding sum of the means of the underlying random variables. If its component underlying variables are uncorrelated, then its variance (mean squared departure from its mean) is the sum of the variances of the underlying processes. If $g(t)$ is a noisy signal composed of superimposed bumps having a common waveform $B(t)$ (zero for $t < 0$) and appearing at a mean rate λ, then the addition-of-means property leads directly to

$$\text{mean } (g) = \lambda \int_0^\infty \mathrm{d}t\, B(t); \tag{1}$$

and, if the bumps are uncorrelated, the addition-of-variances property similarly leads directly to

$$\text{var } (g_u) = \lambda \int_0^\infty \mathrm{d}t\, B^2(t) \tag{2}$$

(the subscript u indicates that $g_u(t)$ is composed of uncorrelated bumps). Eqs. 1 and 2 state Campbell's theorem, which relates the measurable properties mean (g_u) and var(g_u) of the noise $g_u(t)$ to its underlying constituents λ and $B(t)$. Note that the integral in Eq. 1 is the "size" mentioned in the introduction, and that the quadratic integral in Eq. 2 is the size of the variance. If we are dealing with a noisy voltage signal, the physical dimension of $B(t)\ \mathrm{d}t$ is voltage

times time, whereas that of $B^2(t)\ dt$ is voltage squared times time. There is only one way in which the integrals in Eqs. 1 and 2 can be combined to yield a quantity with the physical dimension of voltage, and that is

$$h = \frac{\int_0^\infty dt\ B^2(t)}{\int_0^\infty dt\ B(t)}, \tag{3}$$

whereas

$$T = \frac{\left[\int_0^\infty dt\ B(t)\right]^2}{\int_0^\infty dt\ B^2(t)} \tag{4}$$

is the only combination that dimensionally is a time (Knight, 1973). Eqs. 3 and 4 form natural definitions of the height and duration. Note that h scales linearly with $B(t)$, whereas the same scaling leaves T unchanged. If we choose a rectangular waveform for $B(t)$ and if we call its height h and its duration T, then Eqs. 3 and 4 are identically satisfied. For a bump of arbitrary shape, a reasonable "equivalent rectangular bump" should be such that $h \times T$ equals the bump's exact area, which is manifestly satisfied by Eqs. 3 and 4. If we rescale $B(t)$ to derive a weighting function with unit area, Eq. 3 becomes the average height of $B(t)$ with that weighting. (See Wong et al. [1980] on the distribution of bump sizes.) No reasonable alternative definitions of height and duration will yield numbers drastically different from those yielded by Eqs. 3 and 4 when applied to bumps of reasonable shape.

When Eqs. 3 and 4 are solved for the two integrals, and when the results are substituted into Eqs. 1 and 2, Campbell's theorem takes the simple form

$$\text{mean}\ (g_u) = \lambda h T \qquad \text{and} \tag{5}$$

$$\text{var}\ (g_u) = \lambda h^2 T. \tag{6}$$

If T can be estimated independently by a more detailed scrutiny of the noise signal, then, since mean (g_u) and var (g_u) may be measured directly, Eqs. 5 and 6 can be solved for the underlying λ and h in terms of measured quantities.

Far more general sorts of "superimposed bump" noise can be contemplated; if the mean time-course of the bumps is $B(t)$, Eq. 1 will still hold. Eq. 2 does not have similar generality. However, the bump shape $B(t)$ will always yield the h and T of Eqs. 3 and 4 (and Eq. 5 will follow for general g as a consequence). With some generality, the variance var (g) of the superimposed bump noise should be proportional to the arrival rate λ, and should also depend on the form of the individual bump. The physical dimension of the var (g) is millivolts squared, and the only expression with that physical

dimension, linear in λ (expressed in inverse seconds) and involving h(millivolts) and T(expressed in seconds), is λh^2, as in Eq. 6. Consequently, for more general sorts of superimposed bump noise, the variance can in general be related to its underlying causes through an expression similar to Eq. 6 of the form

$$\text{var } (g) = \psi \lambda h^2 \text{T}, \tag{7}$$

where ψ is a real number without physical dimension, characteristic of the processes that underlie the noise, and where ψ may depart from unity if the assumptions that lead to Eq. 6 do not hold. If ψ as well as T could be estimated by analyzing the noise, then we could obtain h and λ by solving Eqs. 5 and 7, which yield

$$h = \frac{1}{\psi} \frac{\text{var } (g)}{\text{mean } (g)} \quad \text{and} \tag{8}$$

$$\lambda = \frac{\psi}{\text{T}} \frac{[\text{mean } (g)]^2}{\text{var}(g)}. \tag{9}$$

If (contrary to fact) we could collect laboratory records not only of the noise $g(t)$ but also of a second, comparison, noise $g_u(t)$ composed of uncorrelated bumps $B(t)$ with the same values of h and T, arriving at the same λ, then ψ could be measured directly inasmuch as the quotient of Eqs. 6 and 7 is

$$\psi = \frac{\text{var } (g)}{\text{var } (g_u)}. \tag{10}$$

We shall see below that var (g_u), the variance of the comparison uncorrelated bump noise, though not directly measureable, can be estimated from the power spectrum of the correlated bump noise.

We return to the estimation of T for an uncorrelated bump noise $g_u(t)$. Two estimation procedures will be given, both of which utilize the power spectrum, which we now define in terms of the noise autocovariance. The autocovariance $C(\tau)$ of a noise $g(t)$ is formed from the noise departure $g(t) - \bar{g}$ at time t and the departure, a time τ away from t, by forming their product and averaging over t:

$$C(\tau) = \overline{[g(t) - \bar{g}][g(t + \tau) - \bar{g}]}. \tag{11}$$

This experimentally measurable function is a generalization of the variance, because evidently,

$$\text{var } (g) = C(0). \tag{12}$$

The autocovariance may be expressed as a superposition of its frequency components

$$C(\tau) = \int \text{d}f \, S(f) \cos (2\pi f \tau), \tag{13}$$

where the power spectrum $S(f)$, the Fourier coefficient in Eq. 13, can be calculated from $C(\tau)$ by the inverse Fourier formula

$$S(f) = \int d\tau\, C(\tau) \cos(2\pi f\tau). \tag{14}$$

(See Wong et al. [1980]. The more elementary cosine form of the Fourier transformation applies here because, by its definition, Eq. 11, $C(\tau)$ is real and symmetric about $t = 0$, whence $S(f)$ is real and symmetric about $f = 0$.) Eqs. 12 and 13 give

$$\text{var}(g) = \int df\, S(f), \tag{15}$$

which is important below. (The power spectrum more descriptively could be called the "variance spectrum" of g.) Wong et al. (1980) have shown that if $g_u(t)$ is a noise composed of uncorrelated bumps, for which $\tilde{B}(f)$ is the Fourier transform of the bump shape $B(t)$, then

$$S(f) = \lambda |\tilde{B}(f)|^2. \tag{16}$$

Below we shall show that at low light intensity our power spectra support the conclusion that our voltage noise is composed of uncorrelated bumps. For these data, there are two ways in which Eq. 16 can be used to estimate T. The first method simply assumes an analytic form for the bump shape, with parameters to be fit by the power spectrum. Following Fuortes and Hodgkin (1964) and Wong et al. (1980), we choose the form

$$B(t) = \Gamma(t; n, \tau) \equiv \frac{1}{n!\tau} (t/\tau)^n e^{-t/\tau} \tag{17}$$

(we omit a multiplicative amplitude scale because it would not influence T according to Eq. 4). This yields, upon Fourier transformation,

$$|\tilde{B}(f)|^2 = |\tilde{\Gamma}(f; n, \tau)|^2 = \frac{1}{[1 + (2\pi\tau f)^2]^{n+1}}, \tag{18}$$

and, according to Eq. 16, n and τ may be evaluated by fitting this to the scaled experimental power spectrum $S(f)/S(0)$. Then T is evaluated from Eq. 4 by performing the elementary integrals, which yield

$$T = \frac{(n!)^2 2^{2n+1}}{(2n)!} \cdot \tau. \tag{19}$$

The second method for evaluation of T furnishes also some checks on the consistency of the rest of our work; it is a deeper analysis involving the "minimum phase" property, and only a sketch of the procedure is furnished here. Within the set of all waveforms [such as $B(t)$] that might deterministically follow a point event in time [such as a photon absorption or the triggering of $B(t)$] is distinguished a subset of common occurrence: those waveforms with the minimum phase property (see, for example, Page [1955]). There appears to be no single simple characterization of the general physical circumstances that yield this property, but it is easily stated: a waveform is minimum phase if its Fourier transform is the exponential of a causal transfer function. The minimum phase property opens an important computational opportunity:

because the imaginary part of a causal transfer function may be deduced from its real part (by the so-called "Kramers-Kronig analysis" [Kramers, 1927; Kronig, 1936]; see also Titchmarsh [1973] and Page [1955]; Peterson and Knight [1973] give a modern algorithm), knowledge of the amplitude $|\tilde{B}(f)|$ of the Fourier transform of a minimum phase waveform $B(t)$ similarly yields its phase. In turn, amplitude and phase together yield $B(t)$ by inverse Fourier transformation. The bump waveform $B(t)$, if it is minimum phase, can thus be recovered from the measured power spectrum to within a multiplicative coefficient λ according to Eq. 16.

To reconstruct the bump shape from the minimum-phase assertion, we use the power spectrum in dim light to confirm the stronger assertion that the voltage response in dim light is composed of uncorrelated minimum-phase bumps whose waveform is the same as that of bumps measured directly in the dark. First, we determine the shape $B(t)$ of the bump measured in the dark by averaging several samples; the result is shown in Fig. 2 *a*. Then, by Fourier transformation we determine the corresponding amplitude $|\tilde{B}(f)|$. We now postulate the minimum phase property for $B(t)$ and use the resulting algorithm upon $|\tilde{B}(f)|$ to reconstruct the waveform which that postulate predicts; the result is shown in Fig. 2 *b*. The very close agreement with Fig. 2 *a* validates the minimum-phase postulate. None of the numbers generated as described above are used in the next step, which is to postulate Eq. 16 and apply the minimum-phase algorithm again to the independently evaluated experimental power spectrum (extracted from records comparable to the "log $I/I_0 = -5$" line of Fig. 1). The resulting waveform, predicted from the power spectrum alone, is shown in Fig. 2 *c*. The degree of its agreement with the direct waveform measurement of Fig. 2 *a* is strong evidence that the generator potential response to dim light is indeed a superposition of "dark" bumps.

The waveform thus derived from the power spectrum can now be used to numerically evaluate the integrals in Eq. 4, which determine the value of T. The good agreement of this method with the more elementary first procedure justifies that method, which simply fits the two parameters of the waveform Eq. 17 to the experimental power spectrum. (That waveform, in fact, possesses the minimum-phase property.)

Our final largely theoretical task is to show that under bright, steady light the underlying bumps are correlated and to anticipate how this correlation should affect the power spectrum, thereby producing a means for estimating the "adaptation correlation factor," which first appeared in Eq. 7 and which is needed to evaluate h and λ in Eqs. 8 and 9.

Fig. 3, reproduced from Dodge et al. (1968), is an oscilloscope record of the eccentric cell's voltage response to a brief (40-ms) flash superimposed upon a bright, steady light. (The steady-state generator potential amplitude is 16 mV and the response amplitude is ~5 mV.) After its initial rise, the flash-response voltage swings beneath its baseline value and returns to steady state from below. According to the adapting-bump model, the heightened activity early in the record causes a reduction in bump size, and, as a consequence, a reduced voltage response to light later in the record. This reduced voltage is

not the result of a biphasic bump shape: conductance measurements by brief bridge pulses during the flash response revealed that the undershoot conductance was less than the steady-state value, whereas biphasic bumps would have yielded a larger-than-steady-state conductance (just as a larger-than-resting conductance exists in the undershoot of the biphasic nerve action potential).

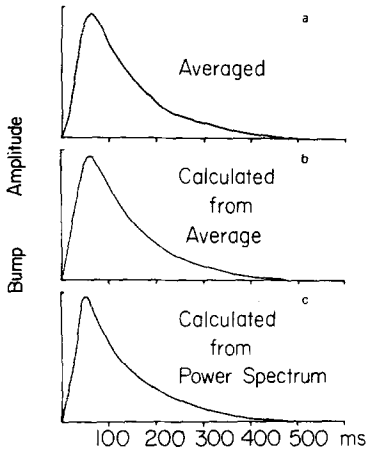

FIGURE 2. The results of calculations based on the minimum-phase assumption. *a* is the average of ten bumps observed to occur spontaneously. They were picked for this analysis because they were clearly seen on the record to be individual bumps and were not picked for their particular shapes. The computer was used to record and average the 10 bumps. The vertical scale is arbitrary since we were only interested in the shape. With this bump shape $B(t)$ the Fourier transform $\tilde{B}(f)$ was obtained. The phase part of this function was ignored, and the phase was calculated instead from the amplitude information by use of the algorithm described by Peterson and Knight (1973). With this and the amplitude information, the bump shape *b* was obtained. That the top two curves are almost identical indicates that the algorithm works for calculating the phase information from the amplitude information, and that our assumption of minimum phase for the bump shape is valid. *c* was obtained by using this same algorithm to calculate the phase information from the amplitude information provided by the power spectrum. The bottom curve looks sharper than the top two curves, but the durations calculated from them differ by only ~10% also indicating that the assumption of minimum phase for the bumps is a good assumption and that the duration of the bumps can be calculated from the power spectrum, as described.

This adaptation is directly related to voltage-generating activity rather than to some other parallel effect of light intensity. It is easily shown that a signal composed of uncorrelated monophasic bumps must yield an autocovariance that is always positive, whereas the experimentally measured autocovariance at bright light (see Fig. 8 of the preceding paper [Wong et al., 1980]) shows a negative-going late phase, which indicates that spontaneous fluctuations of

voltage activity predispose the cell to make a compensating swing to the opposite side of mean activity. A reduction in the size of later bumps due to increased bump release activity would yield the observed effect. (Note that the data quoted in this paragraph and the one before it are also consistent with the alternative hypothesis that bump release activity reduces the likelihood that an absorbed photon will lead to a bump. Data given below will suggest that this indeed is a secondary contributor but not the major mechanism of adaptation.)

The arguments presented above make a substantial case for the response to light being a superposition of bumps whose release activity adjusts itself in a manner appropriately described as "adaptation." If we assume such a model, then Fig. 1 gives some indication as to the time scale over which this

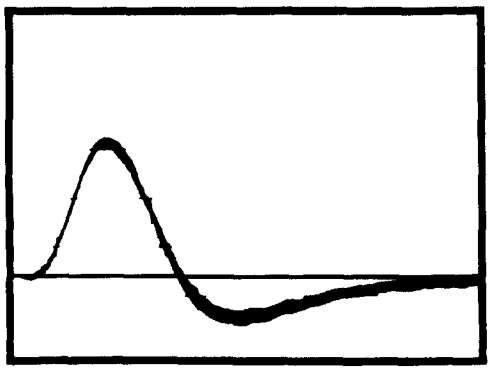

FIGURE 3. Oscilloscope record of the eccentric cell's voltage response to a brief (40-ms) flash superimposed upon a bright, steady light, reproduced from Dodge et al., *Science*, Vol. 160, pp. 88–90, 5 April 1968, copyright 1968 by the American Association for the Advancement of Science. The sweep duration is 0.5 s, and the response amplitude is ~5 mV. The generator potential amplitude is 16 mV.

adaptation occurs. Note that for all light intensities but the lowest there is between light onset and steady state a "transient" period in which the voltage response readjusts downward. This epoch becomes shorter in brighter light, but in all cases its duration is longer than the general time scale of the individual bumps that also can be seen in the figure. This separation between the time scales of bump duration and of adaptation enables us to predict what the effect of adaptation will be upon the power spectrum of the voltage noise.

Adaptation is a "self-correcting" mechanism within the noise that tends to reduce the variance of noise about its mean. The variance is given by the area under the power spectrum (Eq. 15), so the effect of adaptation will be to reduce that area. However, it is a general feature of Fourier representation in terms of frequency components that features which involve only long time scale can affect frequency components only at low frequency. Thus the bump-correlation effect of adaptation upon the power spectrum should be a depression of its low frequency region. (An example of the adapting-bump model, which is analytically solvable in detail, confirms this general argument; see

Appendix.) Figs. 4 (*top*) and 5 show that precisely such a feature is experimentally observed in the power spectrum. In contrast, the power spectrum of a noisy signal composed of uncorrelated monophasic bumps must have its maximum at zero frequency (as follows from Eq. 16).

A method to estimate the adaptation correlation coefficient ψ, which we need for Eqs. 8 and 9, now becomes evident. Inasmuch as correlation influences the power spectrum $S(f)$ at low frequencies, the functional form of Eq. 18 (already validated by its success at low light intensities) can be fitted to the high-frequency end of the power spectrum. This has been done in Fig. 5,

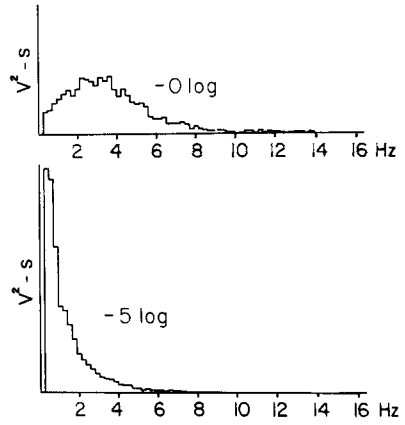

FIGURE 4. The power spectra calculated on transmembrane voltage of *Limulus* retinular or eccentric cells obtained at low light intensity (−5 log) and at high light intensity (0 log). The horizontal axis is frequency and the scale is 0.234 Hz per bin. The vertical scale is in arbitrary units for the power spectrum. The areas under the two curves are normalized. It can be seen that the shapes of the two curves are very different. For low light intensity, the power spectrum is represented by a monotonic curve, whereas for high light intensity, the power spectrum shows a low frequency cutoff due to "adaptation" (see text).

where the smooth curve comes from Eq. 18. The smooth curve "fills up the low frequency notch" and gives an estimate for (say) $S_u(f)$, the power spectrum which would result from fixed uncorrelated bumps of the same average shape as the real correlated ones. With $S_u(f)$ now known, we may twice use Eq. 15 in Eq. 10 to obtain

$$\psi = \frac{\int df S(f)}{\int df S_u(f)}, \tag{20}$$

the ratio of the two areas. Our fitting also yields T from Eq. 19, so that we may now use Eqs. 8 and 9 to evaluate the h and λ.

MATERIALS AND METHODS

Biological Preparations

These experiments were performed on seven eccentric cells of *Limulus*. The cell preparation and general experimental techniques were the same as those described previouslv (Wong et al., 1980).

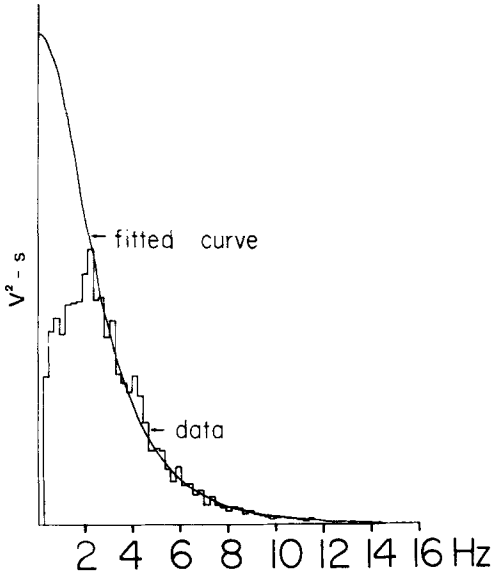

FIGURE 5. The procedure for estimating at high light intensity the duration of the bumps and the adaptation factor ψ. The horizontal scale is frequency in 0.234 Hz per bin and the vertical scale is arbitrary units of power density. The fitted curve (from Eq. 18) was matched to the data at frequencies above ~2 Hz. The areas of the two curves in this range are normalized. Values of the parameters for the best fitted curve were used to calculate the duration from Eq. 19. As described in the text, the ratio of the areas under the two curves (starting from the lowest frequency component) gives an estimation for ψ. The fitted curve corresponds to $n = 1$ and $\tau = 40$ ms in Eq. 19, and the duration calculated from these values was 160 ms. ψ was 0.6.

Data Collection

The transmembrane voltage response to steady light furnishes the data for this investigation. Recording procedures were the same as those described by Wong et al. (1980) except that the episode lengths for light intensities corresponding to −3 log and −2 log were 90 s and those for −1 log and 0 log were 120 s. The −5 log filter furnished a "threshold" generator potential response in the sense that −6 log yielded isolated bumps, separated by intervals of resting potential.

Data Analysis

EVALUATION OF POWER SPECTRA The power spectrum at each light intensity was calculated from data in the steady state. After removal of slow drift, direct

evaluation by averaging squared Fourier coefficients was used, as described in the previous paper (Wong et al., 1980). Fig. 4 shows the power spectrum calculated from data obtained at low light intensity (−5 log) and at high light intensity (0 log). The areas under the two power spectra have been normalized to a common value because this facilitates the visual comparison of spectra taken at different light intensities. It is evident that the shapes of the two curves are very different.

CONFIRMATION THAT MINIMUM PHASE DARK BUMPS UNDERLIE RESPONSE TO DIM LIGHT From a stretch of voltage record taken in the dark, ten consecutive, clearly visible, single, spontaneous bumps were chosen and were averaged with their times of steepest rise in register. The resultant average bump is shown in Fig. 2 *a*.

The Fourier transform of this bump shape was evaluated numerically and converted to its absolute value $|\tilde{B}(f)|$, which was then input to a minimum phase numerical algorithm (Peterson and Knight, 1973). The phase thus calculated was composed with $|\tilde{B}(f)|$, to construct a full minimum-phase Fourier transform to which a numerical inverse Fourier transformation was applied. The resulting minimum-phase waveform is shown in Fig. 2 *b*. Its very close agreement with Fig. 2 *a* demonstrates that the experimentally measured average dark bump likewise has the minimum-phase property.

The −5 log power spectrum of the same cell was then processed with the identical procedures used upon $|\tilde{B}(f)|$. The result, scaled to the same maximum height, is shown in Fig. 2 *c*. It is close to what we would predict if the power spectrum were that of a shot noise of superimposed uncorrelated copies of the minimum-phase bump shape shown in Fig. 2 *a*. The duration parameters T numerically evaluated from Eq. 4 for the waveforms of Fig. 2 *a* and *c* differ by only 10%.

EVALUATION OF DURATION T AND ADAPTATION CORRELATION FACTOR ψ Power spectra at low light intensity (−5 log, −4 log) were fit directly to the functional form of Eq. 18. This was facilitated by comparing a log vs. log presentation of the data against template curves, which yields n and τ together and at once. The duration T was then calculated directly from Eq. 19. The amplitude scale of the raw power spectrum never enters into this procedure. Fitting was done by eye; though this permits substantial flexibility in "plausible" choices of n and τ, these correlated uncertainties largely cancel in Eq. 19, and for every spectrum the most extreme plausible resulting values of T differed by <20%. The values of T independently derived from three cells by the minimum-phase method described above fell within this modest uncertainty and thus supported this simple method for estimating duration. For the example shown in Fig. 4 (*bottom*) the estimated duration is 360 ms.

At higher light intensity, adaptation affects the low-frequency end of the power spectrum, but in such a way that Eq. 18 may still be fit unambiguously to the spectrum at higher frequencies. T may be calculated from Eq. 19 as before. Moreover, according to Eq. 2, the value of the adaptation correlation factor ψ is given by the ratio between the area under the experimental power spectrum and the area under the curve fitted to the higher frequency data. This procedure, again, is independent of the power spectrum's vertical scale.

In Fig. 5 the smooth fitted curve corresponds to $n = 1$ and $\tau = 40$ ms. The resulting duration is T = 160 ms. The ratio of the two areas gives $\psi = 0.6$.

EVALUATION OF HEIGHT h AND RATE λ The height and rate parameters depend upon the absolute scales of the mean and variance of the underlying process. Because the bump process is in the membrane shunt conductance, we must perform a transformation upon our voltage data, as has been discussed in detail by Martin (1955). If the cell's resting conductance is G_0 and if its resting potential is removed

from its equilibrium by a voltage difference E, then a voltage departure V from resting is related to shunt conductance g by the relation

$$\frac{g}{G_0} = \frac{1}{1 - \frac{V}{E}} - 1. \tag{21}$$

If the equilibrium potential is distant from the momentary voltage by a factor several times larger than the fluctuations in the voltage, then we need not use Eq. 21 at each time point; it can be straightforwardly shown that mean and variance of g are approximately related to mean and variance of V by

$$\text{mean } (g/G_0) = \text{mean } (V/E) \left[\frac{1}{1 - \text{mean } (V/E)}\right] \tag{22}$$

$$\text{var } (g/G_0) = \text{var}(V/E) \left[\left(\frac{1}{1 - \text{mean } (V/E)}\right)^4\right], \tag{23}$$

where the brackets enclose the "Martin corrections" to the naive results which would hold if g and V were linearly related. Eqs. 8 and 9 for height and rate thus yield

$$h/G_0 = \frac{1}{\psi} \frac{\text{var } (g/G_0)}{\text{mean } (g/G_0)} = \frac{1}{\psi} \frac{\text{var } (V/E)}{\text{mean } (V/E)} \left[\left(\frac{1}{1 - \text{mean } (V/E)}\right)^3\right] \tag{24}$$

$$\lambda T = \psi \frac{[\text{mean } (g/G_0)]^2}{\text{var } (g/G_0)} = \psi \frac{[\text{mean } (V/E)]^2}{\text{var } (V/E)} \{[1 - \text{mean } (V/E)]^2\}. \tag{25}$$

The summary Fig. 6 shows that at brightest light the rate λ falls below its linear extrapolated value by a factor of about 35, and we may ask if errors in measurement entered into Eq. 25 might account for this factor. This typical cell had a resting potential of $E = 55$ mV, while at the 0 log light it gave mean $(V) = 23.6$ mV. Thus, the correction enclosed in braces in Eq. 25 was about one-fourth, while ψ was about one-third. Even if these two factors were entirely spurious, their removal would fail by a factor of about 3 to lift the rate to its extrapolated value. The modestly sublinear trend in rate with light intensity thus appears to be more than any plausible error in our computational procedure. (The effect of the cell membrane's shunt capacitance upon the accuracy of these procedures must be slight: the cell's resistance-capacitance time constant of no more than $\tau_m = 10$ ms can substantially affect the voltage variance only through that part of the power spectrum that lies above $f = 1/(2\pi\tau_m) \approx 15$ Hz and the power spectrum has already dropped to a small value before that frequency.)

RESULTS AND CONCLUSIONS

Fig. 6 shows calculated values of ψ, T, λ, h plotted across five decades in light intensity. These results are for the cell that yielded the raw data of Fig. 1 and the power spectra shown in Figs. 4 and 5, and are typical of all cells. This cell had a resting potential of -55 mV and a resting resistance of 8 MΩ.

The calculated λ is linear with light intensity through about 500 bumps per second, from a threshold of about 10 bumps per second, but falls behind strict proportionality at higher light intensity until at the brightest light it has fallen a factor of about 35 below the factor of 10^5 extrapolated from threshold. T decreases by a factor of 2 from its threshold value as the light becomes

brighter; though this total drop in duration was similar for all cells, the intensity decade in which the partial drop was greatest proved the most variable feature among our seven cells. ψ descends from unity (which indicates no correlation) in dim light down to one-third in the brightest light. Thus, both T and ψ undergo changes that are extremely modest in comparison with

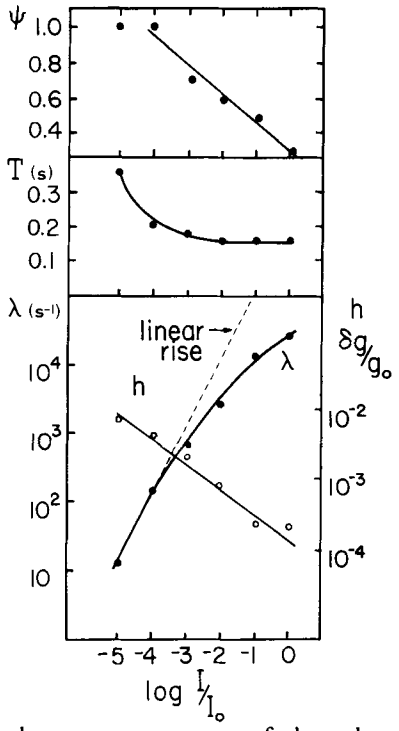

FIGURE 6. The steady-state parameters of the adapting-bump model have been evaluated over a large range of light intensities for a typical eccentric cell. The rate increases proportionally to light intensity up to ~500 bumps/s, and then it departs from strict proportionality. The height, expressed as the fractional increase in conductance in terms of the dark value of total conductance, decreases like the −0.4 power of light intensity. The duration decreases by a factor of 2. The adaptation factor ψ is 1 for the −5 log and −4 log light intensities, indicating that the correlating of the sizes of the bumps did not substantially affect the variance. At higher light intensities, the correlation of sizes of the bumps reduced the variance. At 0 log, ψ was 0.3. (Note that in the top frame, the vertical scale for adaptation factor is truncated well above ψ = 0.)

the changes in light intensity; this fact accounts for the reasonable agreement of our data with the early result of Dodge et al. (1968), where the effect of ψ was not separated from that of T. Across the entire range of light intensity, h descends smoothly as the −0.4 power of the illumination. (This agrees with the original data of Dodge et al. (1968): their quoted −0.5 power resulted from plotting their end point at 0 log intensity one decade too low.)

The height and duration at the dimmest (−5 log) light intensity shown in Fig. 6 agree with estimates made directly from individual spontaneous bumps recorded in the dark. As shown in Fig. 2 *a* and *b*, the average spontaneous bump has a shape with the minimum-phase property; if that property and independence of bump events are postulated for the voltage noise at −5 log light intensity, then the power spectrum predicts a bump shape that agrees well with that observed in the dark, with no further assumptions, as Fig. 2 *c* shows.

The results presented here can be compared directly with the classic study of Fuortes and Hodgkin (1964). These authors explored the basic idea that in *Limulus* the change in time scale may be causally related to the change in sensitivity and observed that a 200-fold reduction in sensitivity was associated with a factor of two decrease in time scale of the response. This observation may be directly related to Fig. 6, which shows a 200-fold reduction in the bump size (height times duration) concurrent with a decrease of a factor of 2 in the duration of the bumps. Over the same span of light intensities there is also a decrease of a factor of about 2 in the time scale of the latency process (Wong et al., 1980).

At the brightest (0 log) light intensity Fig. 6 gives a bump height parameter of 2×10^{-4} times the cell's resting conductance of near 10^{-7} reciprocal ohms, whence our brightest light yields 2×10^{-11} reciprocal ohms for the smallest observed conductance event. This is about what is reported for individual conductance channels at the neuromuscular junction (Anderson and Stevens, 1973). We observed that an approximately comparable uncalibrated light added to our brightest calibrated light would drive the voltage response into saturation; this we may regard as informal evidence that our bumps result from the roughly synchronized opening of channels with individual conductance of $\sim 10^{-11}$ reciprocal ohms. (Complexities in the detailed equivalent circuit of the eccentric cell make the precision of such an estimate questionable. However, our conclusion is supported more formally by observations on ventral photoreceptors of *Limulus* [Wong, 1978].) If this is the case, Fig. 6 further implies that a bump at threshold light intensity (or spontaneous in the dark) is the consequence of ~100 elementary channels opening together. It is easy to imagine that the modest shortening in T, as light increases, may be due to a better synchronization in the activation of elementary channels as their total number (and presumably the membrane area involved in the formation of a single bump) becomes smaller.

We may go a step further if we postulate that the initial transient to the brightest light in Fig. 1 opens a substantial fraction of all the channels. That transient of 28 mV is about half the full resting potential of 55 mV, which implies that the parallel resistance of all the open channels is $\sim 10^7$ Ω; at 10^{11} Ω per channel this implies 10^4 open channels, or a few times 10^4 channels total if a substantial fraction are opened at the transient.

In Fig. 6, at the brightest steady light, there are 2×10^4 events per second; if each event is due to a single elementary channel which remains open for about 0.2 s as T in the figure indicates, then, if there indeed are 10^4 channels, each channel remains open about half the time. In such a regime it is easy to

imagine strong correlations between the successive openings of each elementary channel, and the measured correlation factor of $\psi = 0.3$ is not unexpected.

It is notable that, even when the photon arrivals are reduced to 0.01 maximum (−2 log units in Fig. 6), the situation shown by Fig. 6 remains so similar to that shown at maximum light. The duration has not changed significantly, and, although the rate is down an order of magnitude, the height has increased nearly an order of magnitude, which implies that the fraction of channel open time decreased only slightly. The correlation factor has moved less than halfway back to its uncorrelated value of unity. These changes in the data may be explained naturally if the major physiological effect of the much lowered photon flux is to permit each effective photon to synchronously activate a "block" of nearly ten times more elementary channels than a photon could reach in the brightest light.

We suggest that the cell membrane may be organized by patches into "functional blocks" of elementary channels, which respond with near uninimity (if they respond at all) to any rhodopsin photoisomerization within the patch, and that the patches or functional blocks grow larger when photon captures become fewer. Adaptation of bump size would be a clear consequence. Such a model carries with it a natural time scale that is measured by the mean time between activations of the patch containing a given elementary channel. Because the patch size may adjust, this time scale may be insensitive to large changes in the rate of photon arrivals. Although this interpretation of our data is not unique, informal support for such a model can indeed be drawn from our power spectrum data. We have mentioned that the suppression of low frequencies in the power spectrum rules out a noise signal composed of monophasic bumps that are uncorrelated; the dip at low frequencies is a natural consequence of correlations among bumps, whence the band of frequencies over which it extends should reflect the natural time scale over which those correlations occur. We can roughly characterize that frequency band by noting the frequency at which the power spectrum has recovered half its measured maximum value. Both the 0 log spectrum of Fig. 4 and the −2 log spectrum of Fig. 5 give a half-recovery frequency of 1.14 Hz, an agreement beyond the accuracy of these measurements. That characteristic frequency had held steady in the face of a factor of 10 change in the rate of bump occurrences and a factor of 100 in the rate of photon arrivals. This experimentally observed insensitivity, of the half-recovery frequency to large changes in other experimental variables which likewise have reciprocal time as their physical dimension, is a strong constraint on the physiological models that we may realistically entertain. Our suggestion of "functional blocks" of elementary channels, which adapt in size according to the frequency of photon arrivals, is evidently able to satisfy the constraint because block size may be adjusted to maintain a steady rate of responses per block.

APPENDIX

Effect of Correlation on the Power Spectrum

Knight (1973) analyzes a fairly broad class of adapting bump models in some detail. His is a special treatment of an even more general analysis done independently in

another context by Celasco and Stepanescu (1977). Here we give Knight's conclusions in our notation; equation numbers with decimal points refer to his publication.

A class of models is presented in which bumps are fixed in temporal shape but of variable height determined by a stochastic law. The power spectrum is derived in Eq. 3.20 as

$$S(f) = S_u(f)\left\{1 + \frac{\bar{s}}{\bar{s}^2}[\tilde{k}(f) + \tilde{k}(-f)]\right\}, \tag{A1}$$

where s is height times duration of the bump; $\tilde{k}(f)$ is related to the correlation between a given bump and its successors and predecessors and may be evaluated once assumptions about the mechanism of correlation are made. Typically, $\tilde{k}(f) + \tilde{k}(-f)$ is negative at low frequencies (it is zero for a Poisson process of uncorrelated bumps), and the frequency range over which it is non-zero is the frequency range over which correlation modifies the power spectrum. Thus, Eq. A1 leads naturally to the estimation procedure shown in Fig. 5 and used in Eq. 20; the fraction to which the expression in braces in Eq. A1 reduces the area under the power spectrum is the adaptation correlation factor ψ.

Simple, explicit results can be obtained from the following model, which is physiologically plausible but not in full accord with our data: the bumps might be the consequence of "transmitter release" from vesicles that subsequently refill to an asymptotic maximum content, with an exponential time-course whose rate constant we call γ. If H_0 is the mean rate at which a typical vesicle is discharged, then by Eq. 3.28 the power spectrum is

$$S(f) = S_u(f)\left\{1 - \left[\frac{H_0(H_0 + 2\gamma)}{2(H_0 + \gamma)^2}\right]\frac{1}{1 + \left(\frac{2\pi}{H_0 + \gamma}f\right)^2}\right\}. \tag{A2}$$

In this model, correlation becomes significant when the release rate H_0 approaches or exceeds the growth rate γ. At each light intensity a reasonable fit to our power spectrum data is given by Eq. A2. However, Eq. A2 gives a correlation half-effect frequency of $f_{1/2} = (H_0 + \gamma)/2\pi$. Thus, if H_0 were proportional to the total bump rate, the half-effect frequency would have a sensitive dependence on bump rate, contrary to our observations. This is in accordance with our conclusion that the insensitivity of the half-recovery frequency to a major change in bump rate sets an informative constraint on the sorts of model that we may consider.

The authors wish to thank Ms. Emily Preslar, Ms. Sharon Silverman, and Ms. Su-Jen Wong for typing the many drafts of this manuscript and for their assistance with the illustrations. Thanks are also due to Dr. Charles F. Stevens for bringing to the authors' attention the work of Celasco and Stepanescu (1977).

This work formed part of a dissertation submitted by F. Wong to The Rockefeller University in partial fulfillment of the requirements for a Ph.D. degree.

This work was supported, in part, by National Institutes of Health grants EY 0188 and EY 01428. F. Wong was supported by a graduate fellowship from The Rockefeller University, New York.

Received for publication 24 April 1978.

REFERENCES

ADOLPH, A. 1964. Spontaneous slow potential fluctuation in the *Limulus* photoreceptor. *J. Gen. Physiol.* **48**:297–322.

ANDERSON, C. R., and C. F. STEVENS. 1973. Voltage clamp analysis of acetylcholine produced end-plate current fluctuations at frog neuromuscular junction. *J. Physiol. (Lond.).* **235:**655–691.

BORSELLINO, A., and M. G. F. FUORTES. 1968. Responses to single photons in visual cells of *Limulus. J. Physiol. (Lond.).* **196:**507–539.

CELASCO, J., and A. STEPANESCU. 1977. Power spectrum of pulse sequences with correlation between pulse shape and pulse separation time. *J. Appl. Physiol.* **48:**3635–3638.

DODGE, F. A., B. W. KNIGHT, and J. TOYODA. 1968. Voltage noise in *Limulus* visual cells. *Science. (Wash. D. C.).* **160:**88–90.

FUORTES, M. G. F., and A. L. HODGKIN. 1964. Changes in time scale and sensitivity in the ommatidia of *Limulus. J. Physiol. (Lond.).* **172:**239–263.

FUORTES, M. G. F., and S. YEANDLE. 1964. Probability of occurrence of discrete potential waves in the eye of *Limulus. J. Gen. Physiol.* **47:**443–363.

HAGINS, W. A. 1965. Electrical signs of information flow in photoreceptors. *Cold Spring Harbor Symp. Quant. Biol.* **30:**403–418.

KIRSCHFELD, K. 1966. Discrete and graded receptor potentials in the compound eye of the fly (*Musca*). *In* The Functional Organization of the Compound Eye. C. G. Bernhard, editor. Pergamon Press Ltd., Oxford. 291–307.

KNIGHT, B. W. 1973. A stochastic problem in visual neurophysiology. *In* American Mathematical Society Symposium on Stochastic Differential Equations. J. Keller and H. J. McKean, editors. American Mathematical Society, Providence, R. I. 1–19.

KRAMERS, H. A. 1927. *Estratto dagli Atti del Congresso Internazionale de Fisici Como. Nicolo Zanichelli, Bologna.* **2:**545.

KRONIG, R. DE L. 1936. *Physica (Utr.).* **3:**1009.

MARTIN, A. R. 1955. A further study of the statistical composition of the end-plate potential. *J. Physiol. (Lond.).* **130:**114–122.

MILLECCHIA, R., and A. MAURO. 1969. The ventral photoreceptor cells of *Limulus.* II. The basic photoresponse. *J. Gen. Physiol.* **54:**310–330.

PAGE, C. H. 1955. Physical Mathematics. D. Van Nostrand Co., Inc. Princeton, N. J.

PETERSON, C. W., and B. W. KNIGHT. 1973. Causality calculations in the time domain: an efficient alternative to the Kramers-Kronig method. *J. Opt. Soc. Am.* **63:**1238–1342.

RICE, S. O. 1944. Mathematical analysis of random noise. *Bell Tel. Syst. J.* **23:**282–332.

SCHOLES, J. 1965. Discontinuity of the excitation process in locust visual cells. *Cold Spring Harbor Symp. Quant. Biol.* **30:**517–527.

RUSHTON, W. A. H. 1961. The intensity factor in vision. *In* Light and Life. W. D. McElroy and H. B. Glass, editors. The Johns Hopkins University Press, Baltimore. 706–722.

TITCHMARSH, E. C. 1937. Introduction to the Theory of Fourier Integrals. Oxford University Press, Oxford. Theorem 95.

WONG, F. 1978. Nature of light-induced conductance changes in ventral photoreceptors of *Limulus. Nature (Lond.).* **276:**76–79.

WONG, F., B. W. KNIGHT, and F. A. DODGE. 1980. Dispersion of latencies and the adapting-bump model in photoreceptors of *Limulus. J. Gen. Physiol.* **76:**517–537.

WU, C. F., and W. L. PAK. 1975. Quantal basis of photoreceptor spectral sensitivity of *Drosophila melanogaster. J. Gen. Physiol.* **66:**149–168.

YEANDLE, S. 1957. Studies on the slow potential and the effects of cation on the electrical responses of the *Limulus* ommatidium. Ph.D. thesis, The Johns Hopkins University, Baltimore.